Optical fine structures of highly quantized InGaAs/GaAs self-assembled quantum dots

H. Y. Ramirez,[1] C. H. Lin,[1] C. C. Chao,[1] Y. Hsu,[1] W. T. You,[1] S. Y. Huang,[1] Y. T. Chen,[1] H. C. Tseng,[1] W. H. Chang,[1] S. D. Lin,[2] and S. J. Cheng[1,*]

[1]*Department of Electrophysics, National Chiao Tung University, Hsinchu 30050, Taiwan*

[2]*Department of Electronic Engineering, National Chiao Tung University, Hsinchu 30050, Taiwan*

(Received 8 February 2010; revised manuscript received 14 June 2010; published 30 June 2010)

A theoretical model for the electron-hole exchange interaction in three-dimensionally (3D) confining semiconductor nanostructures is presented to explain the observed decreasing tendency of the fine-structure splittings (FSSs) of small InGaAs/GaAs self-assembled quantum dots (QDs) with increasing the emission energies. The experimentally revealed FSS reduction is shown to be highly associated with the significant 3D spreading of electronic orbitals and reduced overlap of electron and hole wave functions in small and/or Ga-diffused QDs. The combination of quantum size and Ga-diffusion effects substantially reduces the averaged *e-h* exchange interaction and leads to the reduced FSSs in the regime of high emission energy.

DOI: 10.1103/PhysRevB.81.245324 PACS number(s): 71.70.Gm, 78.67.Hc, 78.55.Cr

I. INTRODUCTION

The fine-structure splittings (FSSs) of spin excitons (Xs) in quantum dots (QDs) have been confirmed as a main obstacle for the fabrication of dot-based entangled photon pair emitters, a key device required in optical quantum teleportation and cryptography.[1–4] The FSS between the spin bright X states of a QD is widely believed as the consequence of the part of *e-h* exchange Coulomb interaction arising from the inevitable symmetry breaking of dot structure due to, for instance, shape elongation or strain.[5,6] To make the generation of entangled photon pair from a QD feasible, the optical FSSs are required to be smaller or at least comparable to the intrinsic broadening of X emission line, typically at the scale of ~ 1 μeV.[7–9] In reality, the magnitudes of FSSs of self-assembled QDs (SQDs), however, vary from dot to dot in a wide range of 10^0-10^2 μeV and mostly are larger than the optical intrinsic broadening.[10–14]

Experimentally, the measured FSSs of self-assembled QDs are often shown to decrease with the increasing emission energy, and sometimes even drop into the scale comparable to the intrinsic broadening of X emission lines in the high-energy regime.[15–17] Such an observed feature suggests the usefulness of smaller dots. However, the underlying physics of the useful feature remains a puzzling subject. In a simple picture, the FSSs of smaller dots are actually expected to be larger, rather than nearly vanishing as observed because reducing the QD size increases the local density of confined charged particles and the strength of the *e-h* exchange interaction as well.

Seguin *et al.*[16] explains such an anomalous energy dependence of FSS in terms of the effects of strain-induced piezoelectricity (PZ). Their studies show that the PZ in QDs breaks the *e*- and *h*-wave-function symmetry and increases the FSSs. Because the PZ is more significant in larger dots, the observed FSSs show a decrease with reducing dot size. By contrast, the shape asymmetry of QDs was shown mostly as a secondary effect and becomes crucial only in very small QDs.

The roles of strain and shape asymmetry in the optical fine structures of QDs were further distinguished by Abbarchi *et al.*[17] in their recent study of unstrained GaAs/AlGaAs QDs fabricated using the technique of droplet epitaxy (DE). In spite of lacking of strain and PZ, still similar feature of FSS as a function of the emission energy was observed. The study evidences the crucial role of shape asymmetry in the FSSs of DE-grown QDs, which usually show a close correlation between lateral shape elongation and QD size.

In this work we present experimental and theoretical studies of optical FSSs of a series of small InGaAs/GaAs QDs emitting lights at high energies ranging from 1.34 to 1.39 eV. The PZ effect is negligible in such small dots. Nevertheless, a distinct monotonic decrease in the measured FSSs for a series of the QDs with increasing the emission energies is observed.

A theoretical model for the *e-h* exchange interaction in three-dimensionally (3D) confining semiconductor nanostructures is presented to explain the observed decreasing tendency of the FSSs. Our studies establish that, besides the widely discussed effects of PZ and the possible elongation-size correlation,[18] quantum size effects and the resulting small *e-h* wave-function overlap play also significant roles in the reduced FSSs of small InGaAs/GaAs QDs.

The paper is organized as follows. Section II presents the experimental data of polarized photoluminescence (PL) spectra and the optical fine structures of individual QDs. Section III presents the developed theoretical model for the *e-h* exchange interactions and the numerical simulation for the electronic structures of QDs. Section IV shows our analysis of the theoretical and experimental results. Section V provides the conclusion.

II. EXPERIMENTAL OBSERVATIONS

The investigated QD of sample was grown on a GaAs (001) substrate by molecular-beam epitaxy. A layer of InAs self-assembled QDs was formed by depositing 2.0 monolayers of InAs on GaAs at 480 °C without substrate rotations, yielding a gradient in dot density on the wafer ranging from 10^8 to 10^{10} cm^2. Finally, an undoped capping GaAs layer was deposited on the dots. The average size of uncapped QDs has been identified by atomic force microscopy (AFM),

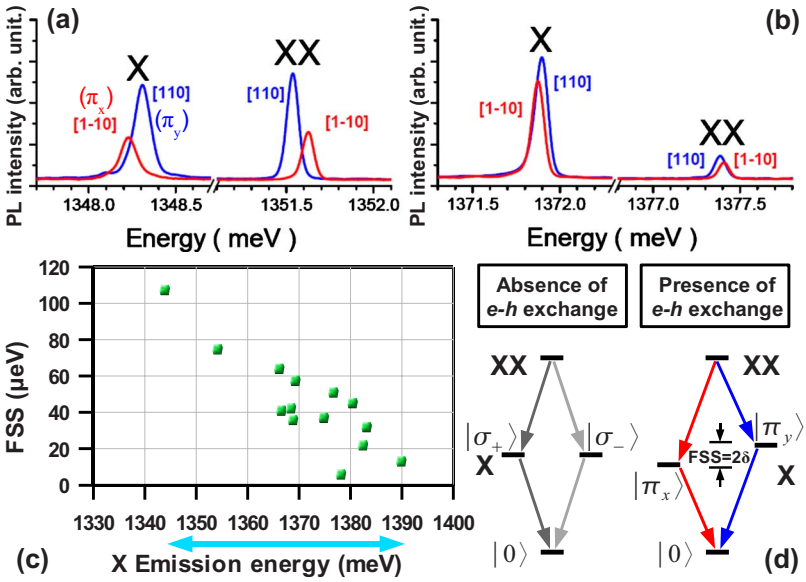

FIG. 1. (Color online) (a) and (b) Polarized PL spectra taken from two single QDs at $T=5$ K with polarization directions along [110] and $[1\bar{1}0]$. Peaks corresponding to X and XX recombination are identified according to the power dependences of their intensities. (c) The measured FSSs as a function of X emission energy for 14 quantum dots (the horizontal line with double arrows lying below the horizontal axis highlights the spectral range of the measured emission energies), and (d) schematic diagrams of XX-X cascade decay in the absence and presence of the *e-h* exchange interaction, respectively.

showing ≈ 15 nm in diameter and $\approx 2 \pm 0.5$ nm in height. However, after a capping layer is grown, the size of a capped QD is usually further reduced by few nanometers. An aluminum metal mask with electron-beam patterned apertures arrays ($\varphi 0.3$ μm), was used to measure emission spectra from individual QDs. The microphotoluminescence setup includes an He-Ne laser beam focused onto the aperture via a microscope objective (N.A.$=0.5$). The PL signals were collected by the same objective lens, analyzed by a 0.75 m grating monochromator and detected by a liquid-nitrogen-cooled charge-coupled device camera, which yields a resolution-limited spectral linewidth of about 60 μeV. We enhance the accuracy to determinate peak position of emission lines by using the Lorentzian line-shape analysis. Thus, peak position resolution is reduced to <10 μeV.

Figures 1(a) and 1(b) show a pair of typical polarized PL spectra taken from two single QDs at $T=5$ K with polarization directions along $[1\bar{1}0]$ and [110], which are set as the x and y axis, respectively, in this work. Emission lines corresponding to X and biexciton (XX) recombination have been identified according to their linear and quadratic power dependencies of intensities.[19] In Figs. 1(a) and 1(b), the X lines consist of linearly cross-polarized (π_x and π_y) doublets with the fine-structure splittings (FFS$\equiv |E_X(\pi_y) - E_X(\pi_x)|$) of about 100 μeV and 20 μeV, respectively. The FSSs of XX are the same as those of X but with a reversed polarization sequence, indicative of a cascade recombination process from the XX to the X states. The lower energy X lines and the higher energy XX lines are polarized along the $[1\bar{1}0]$ direction, in agreement with other studies.[15,20]

Figure 1(c) shows the measured FSSs for all investigated QDs as a function of their X emission energies. A clear decreasing tendency of the measured FSSs with increasing the emission energy is observed. The emission energies from the measured dots are high and distribute in a narrow spectral range from 1320 to 1400 meV, as highlighted by a horizontal double arrow line in Fig. 1(c). The measured dots are thus speculated to have the same height but slightly varied lateral sizes and/or Ga composition. Similar energy dependences of optical FSS were observed also in the previous studies of larger strained InGaAs/GaAs self-assembled QDs,[16] and unstrained GaAs/AlGaAs SQDs.[17] The similar feature observed here for the measured small strained QDs, however, cannot be completely understood in terms of the PZ effect for large InAs/GaAs QDs, nor the size-elongation correlation for unstrained GaAs/AlGaAs QDs as in Refs. 16 and 17, respectively. To capture the main underlying physics, a 3D finite-difference simulation for the electronic structure of strained QDs and a theoretical model for the *e-h* exchange interaction of 3D confining QDs are presented as follows.

III. THEORETICAL MODEL

First, the electronic structures of strained InGaAs/GaAs QDs are examined by performing a 3D finite-difference simulation. We consider truncated-pyramid-shaped $In_{0.67}Ga_{0.33}As/GaAs$ QDs with fixed height of $L_z = 1.8$ nm but various lengths of base (L_x, L_y). The 3D Schrödinger equations for a single electron or a single hole are separately solved in the single-band effective-mass approximation. The strain in a QD is calculated using finite-element method,[21] and considered in the determination of the interband energy gap and the band-edge offsets between dot and barrier. The Ga interdiffusion has been considered in the strain simulation. The strain parameters are modeled as smooth functions of the composition and position following the formula in Ref. 22

The high measured emission energies shown in Fig. 1 could be caused, besides the small sizes of QDs, also by the increased energy-band gap by Ga diffusion. We model the In-Ga interdiffusion between dot, capping layer, and substrate using one-dimensional Fick's theory and describe the Ga- or In-composition profiles using a complementary error function with the characteristic diffusion length l_D.[23,24]

To better focus on the size and diffusion effects, we first fix the lateral elongation to the constant value $\Xi = 95\%$ for the considered QDs in Figs. 2–4. [The results for the QDs with different shape elongations ($\Xi = 98\%$ and 95%) will be

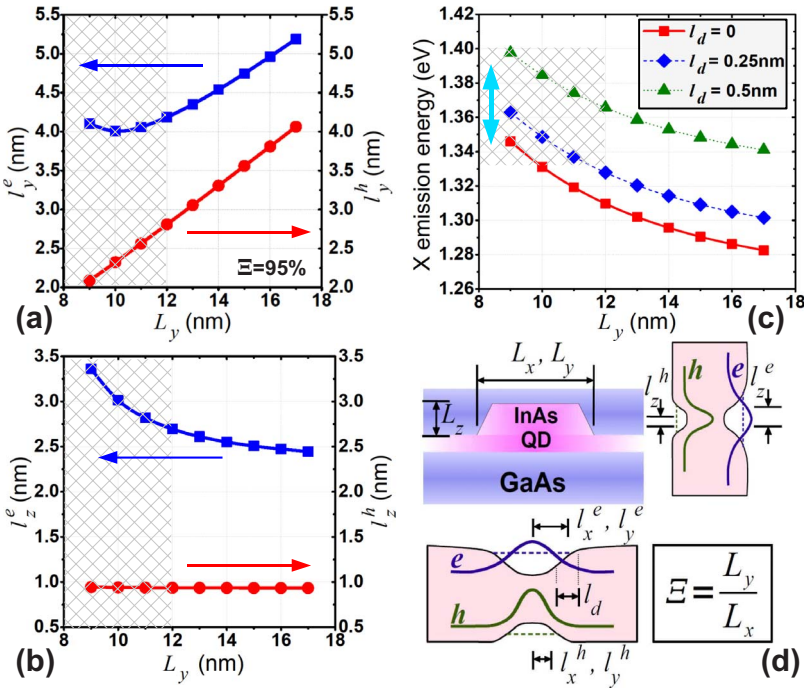

FIG. 2. (Color online) (a) Lateral e (blue squares) and h (red circles) wave-function extent ($l_y^{e/h}$). (b) Vertical e (blue squares) and h (red circles) wave-function extent ($l_z^{e/h}$). (c) Emission energies as functions of the lateral size for different diffusion lengths. The vertical cyan solid line with double arrows indicates the observed spectral range of light emission from the dots. Accordingly, the lateral sizes of the measured dots are speculated to distribute in the hatched region. (d) Schematic depiction of a truncated-pyramid-shaped QD considered in simulation and the relevant defined parameters.

presented and discussed later in Fig. 5.] Figures 2(a) and 2(b) show the calculated extent $l_\alpha^{e/h} \equiv \sqrt{2}\langle\alpha^2\rangle^{1/2}(\alpha = x, y, z)$ of the particle (e or h) wave functions in the lowest orbitals of the QDs with different base lengths from $L_y = 9$ to 17 nm. Figure 2(c) shows the calculated emission energies as functions of the dot size. Comparing the simulated results of Fig. 2(c) and measured emission energies, the measured dots are speculated to have the lateral sizes between 9 and 12 nm (see the hatched region), consistent with the observation of AFM and measured diamagnetic shifts by magnetophotoluminescence measurement.[25] In this regime, the energy level of the lowest electronic orbital is raised by strong energy quantization so much as to be very close to the extended continuum states of wetting layer. It turns out that the electron wave-function extents become surprisingly large in the small dots and very sensitive to the varying of QD size [see l_y^e shown in Fig. 2(a) for $L_y < 12$ nm]. In particular, the wave-function extent in the growth (z) direction is shown even more sensitive than the lateral extent in such small QDs [see l_z^e shown in Fig. 2(b) for $L_y < 12$ nm]. This suggests the necessity of a 3D model for the e-h exchange interactions of the highly quantized small QDs.

The fine-structure splitting (FSS$=2\delta$) between bright X states of a QD is mainly determined by the long-range part of e-h exchange interaction defined as

$$\delta \equiv \int\int d^3r_1 d^3r_2 [\rho_{\Downarrow\uparrow}^{eh}(\vec{r}_2)]^* \frac{e^2}{4\pi\varepsilon_0\varepsilon r_{12}} \rho_{\Uparrow\downarrow}^{eh}(\vec{r}_1), \qquad (1)$$

where $\rho_{\chi\sigma}^{eh}(\vec{r}_1) \equiv [\Psi_0^h(\vec{r}_1)u_{v\chi}(\vec{r}_1)]^* \times \Psi_0^e(\vec{r}_1)u_{c\sigma}(\vec{r}_1)$ is defined as the charged density of e-h transition, $\sigma = \uparrow/\downarrow (\chi = \Uparrow/\Downarrow)$ stands for the up/down spin of electron (valence heavy hole) with spin projection $s_z = \frac{+1}{2}/\frac{-1}{2}$ ($j_z = \frac{+3}{2}/\frac{-3}{2}$), respectively, $\Psi_0^e(\Psi_0^h)$ is the envelope wave function of the lowest orbital for electron (hole), and $u_{c\sigma}(u_{v\chi})$ is the corresponding conduction (valence) band Bloch function. The valence hole here is assumed to be a pure heavy hole for highly quantized and strained self-assembled QDs. The considered bright X states are the e-h pairs with opposite electron and hole spins, i.e., $|\Uparrow,\downarrow\rangle$ or $|\Downarrow,\uparrow\rangle$, of total angular momentum $M = +1$ or -1, respectively.[10,26,27] In principle, the long-ranged e-h exchange interaction δ can be evaluated by substituting the numerically calculated e- and h-wave functions into the standard definition above and numerically carrying out the six-dimensional integration.

Here, in order to gain more physical insight into the problem, a theory based on a 3D asymmetric parabolic model is employed for the evaluation, which provides an explicit generalized formulation of e-h exchange interactions transparently in terms of relevant material properties, wave-function extents, and lateral elongation for an asymmetric QD. Via the fitting of wave-function extents, $l_\alpha^{e/h}$, the wave functions of the lowest orbitals of asymmetric QDs can be modeled by Gaussian functions $\Psi_0^{e/h}(\vec{r}) = (\frac{1}{\pi^{3/2} l_x^{e/h} l_y^{e/h} l_z^{e/h}})^{1/2} \exp\{-\frac{1}{2}[(\frac{x}{l_x^{e/h}})^2 + (\frac{y}{l_y^{e/h}})^2 + (\frac{z}{l_z^{e/h}})^2]\}$. In the analysis, the Coulomb integration is decomposed into a large number of dipole-dipole interactions between the microscopic e-h transition densities of different unit cells and derived as the summation of all these possible interactions over the whole spatial region of QD. After some algebra, the long-ranged e-h exchange interaction is derived for slightly laterally deformed dots as

$$\delta = K \cdot \beta \cdot \xi(1-\xi) \cdot \frac{\gamma_z}{(l_y^{eh})^3}, \qquad (2)$$

where the form factor $K = \frac{3\sqrt{\pi}e^2\hbar^2 E_p}{(4\pi\varepsilon_0)16\sqrt{2}\varepsilon m_0 (E_g^b)^2}$ is given in terms of universal constants and relevant material parameters (including the conduction-valence-band interaction energy E_p, the bulk energy gap E_g^b, and the dielectric constant ε), and

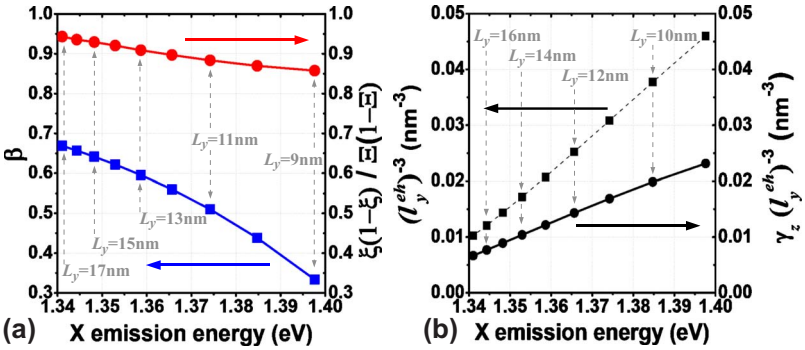

FIG. 3. (Color online) (a) Parameters of *e-h* wave-function overlap β (blue squares), and lateral elongation of wave function normalized by dot shape elongation $\frac{\xi(1-\xi)}{\Xi(1-\Xi)}$ (red circles), as functions of the emission energy. (b) Inverse cubic power of the average in-plane interaction distance $(l_y^{eh})^{-3}$ (dashed line with squares), and damped inverse cubic power of the in-plane interaction distance $[\gamma(l_z^{eh})(l_y^{eh})^{-3}]$ (solid line with circles). A diffusion length l_D=0.5 nm is considered here.

$$l_\alpha^{eh} \equiv \frac{\sqrt{2} l_\alpha^e l_\alpha^h}{\sqrt{(l_\alpha^e)^2 + (l_\alpha^h)^2}}, \tag{3}$$

is defined as the characteristic extent of the hybridized *e*- and *h*-wave function of X in the direction $\alpha = x, y, z$,

$$\beta \equiv \beta_x \cdot \beta_y \cdot \beta_z = \left[\frac{2(l_x^h/l_x^e)}{1+(l_x^h/l_x^e)^2}\right]\left[\frac{2(l_y^h/l_y^e)}{1+(l_y^h/l_y^e)^2}\right]\left[\frac{2(l_z^h/l_z^e)}{1+(l_z^h/l_z^e)^2}\right], \tag{4}$$

is defined to parameterize the *e-h* wave-function overlap (β=1 as *e*- and *h*-wave functions are perfectly identical). The term $\xi(1-\xi)$ with the defined parameter of wave-function elongation

$$\xi \equiv \frac{l_y^{eh}}{l_x^{eh}} \tag{5}$$

measures the lateral asymmetry of exciton wave function.[26] With the nature of dipole-dipole interaction, the interaction strength of Eq. (2) is scaled as an inverse of the cubic power of the lateral interaction distance $[\delta \propto 1/(l_y^{eh})^3]$ and corrected by a factor $\gamma_z < 1$ due to the finite extent of wave function in the *z* direction. Within the currently used model, the correcting factor is derived as

$$\gamma_z = e^{(3\sqrt{\pi} l_z^{eh}/4 l_y^{eh})^2} \operatorname{erfc}\left(\frac{3\sqrt{\pi} l_z^{eh}}{4 l_y^{eh}}\right). \tag{6}$$

The value of γ_z is γ_z=1 for an ideal two-dimensional (2D) dot and decreases ($\gamma_z < 1$) with the increasing aspect ratio l_z^{eh}/l_y^{eh}. As compared with previous relevant theories,[26,28] the derived Eq. (2) provides an extended formulation of the *e-h* exchange interaction with the further consideration of 3D features of asymmetric *e*- and *h*-wave-function extents, and is suitable for the application of 3D confining nanostructures with arbitrary aspect ratios.

For quasi-2D QDs where $l_z^{eh}/l_y^{eh} \ll 1$, Eq. (2) can be expanded as

$$\delta \approx K \cdot \beta_x \beta_y \beta_z \cdot \frac{\xi(1-\xi)}{(l_y^{eh})^3}\left(1 - \frac{3}{2}\frac{l_z^{eh}}{l_y^{eh}} + \cdots\right). \tag{7}$$

In the 2D limit where $l_z^{eh} \to 0$ and β_z=1, Eq. (2) is reduced to the known formulation of long-ranged *e-h* exchange interaction for ideal 2D QDs, as presented in Refs. 26 and 28.

For a strongly confining QD, the attractive *e-h* direct Coulomb interaction in an X can be estimated by the Coulomb matrix element, $V_{eh} = \int\int d^3 r_1 d^3 r_2 \Psi_0^{h^*}(\vec{r}_1)\Psi_0^{e^*}(\vec{r}_2)\frac{e^2}{4\pi\varepsilon_0\varepsilon|\vec{r}_1-\vec{r}_2|}\Psi_0^e(\vec{r}_2)\Psi_0^h(\vec{r}_1)$. In the 3D parabolic model, we derive

$$V_{eh} \approx \frac{e^2}{4\pi\varepsilon_0\varepsilon}\frac{2}{\sqrt{\pi}}\frac{1}{\sqrt{(l^e)^2+(l^h)^2}}\frac{\sin^{-1}\left(\sqrt{1-\left(\frac{(l_z^e)^2+(l_z^h)^2}{(l^e)^2+(l^h)^2}\right)}\right)}{\sqrt{1-\left(\frac{(l_z^e)^2+(l_z^h)^2}{(l^e)^2+(l^h)^2}\right)}}, \tag{8}$$

where $l^e = \sqrt{l_x^e l_y^e}$ and $l^h = \sqrt{l_x^h l_y^h}$. According to Eqs. (2) and (8), the correlation between the averaged energy of polarized emission lines $E_X = E_e + E_h + E_g^b + \Delta E_g^s - V_{eh}$ and the magnitude of the FSS $\equiv |2\delta|$ can be simulated for the QDs considered in Fig. 2.

The following material parameters are used for the strained $In_{0.67}Ga_{0.33}As/GaAs$ QDs considered in this work: E_p=23.3 eV, E_g^b=0.67 eV, the offset of energy gap caused by strain ΔE_g^s=0.23 eV, ε=14.5, dot/barrier valence-band offset V_{vo}=0.24 eV, dot/barrier conduction-band offset V_{co}=0.41 eV, $m_{HH}^* = 0.5 m_0$, $m_e^* = 0.04 m_0$ (dot) and $m_e^* = 0.066 m_0$ (barrier).[29]

IV. RESULTS AND DISCUSSIONS

The expression of Eq. (2) accounts for the possible factors that determine the magnitude of the FSS of a 3D confining QD, including the intrinsic material properties, the lateral elongation of particle wave function [parameterized by $\xi(1-\xi)$], the *e-h* wave-function overlap (parameterized by β), and the mean interparticle distance [related to the quantity $\gamma_z/(l_y^{eh})^3$].[26,28] Figure 3(a) shows the calculated parameter of *e-h* wave-function overlap β and the term of lateral elongation $[\xi(1-\xi)]/[\Xi(1-\Xi)]$, as functions of the X emission energy for the QDs of various sizes. The calculated β values are shown to decrease with the increasing X emission energies. In other words, the *e-h* wave-function overlaps of the dot-confined Xs in the high emission energy regime decrease with decreasing the dot sizes. The value of β is even as low as $\beta \sim 0.35$ for the small dot of L_y=9 nm because of the significant extension of electron wave function (especially in the *z* direction, as mentioned previously). By contrast, the elongation term $\xi(1-\xi)$ remains mostly insensitive

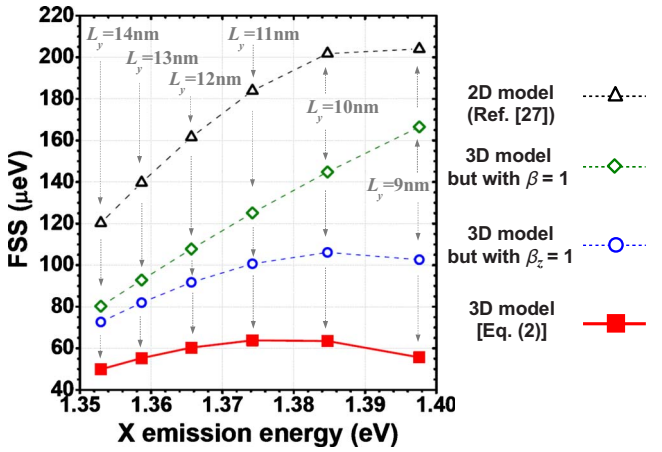

FIG. 4. (Color online) Calculated FSSs ($\equiv|2\delta|$) as a function of the X emission energy obtained by using the full 3D formulation of Eq. (2) (red squares), the 3D formulation but with $\beta_z=1$ set artificially (blue circles), and the 3D formulation but with $\beta=1$ (identical 3D wave functions of electron and hole are assumed and the *e-h* wave-function overlap is 100%) (green diamonds). The result obtained using the 2D model (black triangles) in Ref. 28 is also shown for comparison. A diffusion length $l_D=0.5$ nm is considered here.

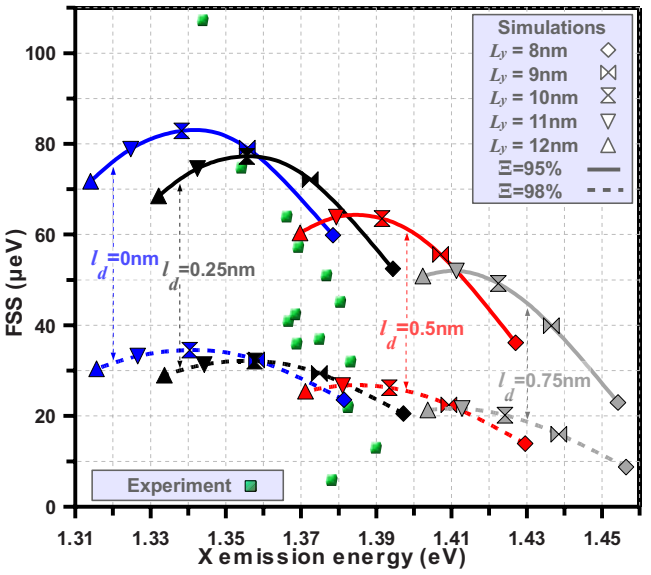

FIG. 5. (Color online) Measured and calculated FSSs of diffused QDs as functions of the X emission energy. Experimental data are shown by green filled squares. Theoretical results are calculated for different dot sizes and diffusion lengths, and are indicated by various kinds of different colored symbols. Solid (Dashed) lines: data for the QDs with the lateral shape elongation, $\Xi=95\%$($\Xi=98\%$).

to the change in dot size because the dominant hole wave function is well localized in the dot. The reduced β substantially reduces the *e-h* exchange interaction, as indicated by Eq. (2).

On the other hand, as shown also by Eq. (2), the strength of the *e-h* exchange interaction is increased by the increase in the quantity $\gamma_z/(l_y^{eh})^3$, i.e., the decrease in the averaged interparticle distance. Figure 3(b) shows that the calculated values of $\gamma_z/(l_y^{eh})^3$ for the same considered dots increase with the increasing X emission energies, showing an opposite behavior of energy dependence to those of β and ξ. Even though the extent of wave function in the z direction is significant and makes smaller the value of γ_z in the regime of small QD, $\gamma_z/(l_y^{eh})^3$ remains increasing with increasing the X emission energy. Thus, if the *e*- and *h*-wave functions were nearly symmetric ($\beta\approx1$) as described by a simplified hard wall model of QD, the FSS of a spin exciton in the dot should increase with reducing the dot size, as observed in most colloidal nanocrystals.[30] However, the FSS of small QDs with finite confining barriers might be suppressed by the strong quantum size effect that leads to the reduced *e-h* wave-function overlap and diminishes the *e-h* exchange interaction in a dot-confined exciton.

Figure 4 shows the calculated FSSs of the considered QDs as a function of the X emission energy. In the low-energy regime ($E_x<1.375$ eV), the FSSs do increase with increasing the energy as expected in a simple hard wall model since both electrons and holes are well localized in the dots. As the dot size is further reduced down to $L_y<12$ nm and $E_X>1.375$ eV, significant delocalization of electron-wave function and the resulting small β make the FSSs turn to decrease with increasing the emission energy. To highlight the effect of reduced *e-h* wave-function overlap, especially that for the vertical wave function in z direction, Fig. 4 presents also the calculated results for the ideal 2D model,[28] for the 3D model [Eqs. (2)–(5)] but with the parameters artificially set as $\beta=\beta_x\beta_y\beta_z=1$, and for $\beta_z=1$ as well, for comparison. We see that, with disregarding the decreasing *e-h* wave-function overlap, the FSSs as a function of the emission energy no longer shows a decreasing tendency in the high-energy regime.

To account for the observed feature of Fig. 1, we calculate the FSSs for QDs of various sizes ($L_y=8-12$ nm), diffusion lengths ($l_D=0,0.25,0.5,0.75$ nm), and shape elongations ($\Xi=95\%$ and $\Xi=98\%$). As shown in Fig. 5, the quantum size effect in the small QDs reduces the FSSs but within a narrow spectral range. With more In-Ga interdiffusion, the FSS of a diffused QD is further reduced while the emission energy is increased. The In-Ga interdiffusion smoothes out the barrier of confining potential and reduces the barrier height so that the particle wave functions become more likely extended into the barrier region. In fact, the electron-wave function is extended more than holes because of the light mass. It turns out that the *e*- and *h*-wave functions become even more different and the *e-h* wave-function overlap smaller in the diffused dots. In addition, the In-Ga interdifussion leads also to the increase in the interband gap and makes the emission energies blue shifted. As a result, the FSSs are further reduced with the increased emission energies by introducing more Ga composition into the dot. The Ga-diffusion effects revealed here could also account for the observed small FSSs of QDs under postannealing treatment in previous studies.[15] As compared with the results for $\Xi=5\%$, the FSSs of the considered QDs with smaller lateral elongation $\Xi=2\%$ retain the similar decreasing dependence on the emission energy but are in the smaller range of FSS magnitude between 10 and 35 μeV.

This model calculation provides us a qualitatively physical understanding of the main observed feature. It points out

the significant roles of quantum size and Ga interdiffusion in the decreased fine-structure splitting of small quantum dots. Nevertheless, the calculated FSSs show a slower decrease with increasing the emission energies as compared with the experimental data. The further decrease in FSS might be attributed to the neglected effects in the model, such as piezoelectricity, size-elongation correlation, or heavy- and light-hole mixing.[27] It is possible to extend the employed model by including piezoelectric potential in the model calculation and using multiband theory to consider the mixing of heavy- and light-hole components in the exciton states to figure out the remaining discrepancy.

V. SUMMARY

In conclusion, we have presented a theoretical and experimental study of optical fine structures of highly quantized $In_{1-x}Ga_xAs/GaAs$ self-assembled quantum dots. A theoretical model for the electron-hole exchange interaction in three-dimensionally confining nanostructures is presented to explain the observed substantially reduced fine-structure splittings of the measured QDs in the regime of high emission energy. The reduced FSSs are attributed to the quantum size and interdiffusion effects of the small dots, leading to the formation of weakly confined electron wave functions. The delocalization of electron-wave function is especially significant and size sensitive in the growth direction and results in the substantially reduced overlap of electron- and hole-wave functions of exciton. The quantum size effect reduces the averaged *e-h* exchange interaction and leads to the decreased FSSs in the regime of high emission energy. Introducing more Ga composition into a dot via In-Ga interdiffusion makes the electron wave function even more extended and the emission energy blueshifted. The model calculation identifies the significant roles of quantum size and Ga interdiffusion in the decreased fine-structure splitting of small quantum dots. Quantitatively, the calculated FSSs, however, show a slower decrease with increasing the emission energies as compared with the experimental data. The further decrease in the fine-structure splittings of the QDs in the regime of high energy $\sim$1.39 eV could be related to other mechanisms beyond the treatment of the model, e.g., piezoelectricity, size-elongation correlation, and mixing of heavy- and light-hole component, and remains an interesting subject for further study.

ACKNOWLEDGMENTS

The authors acknowledge the National Science Council of Taiwan for financial support under Contract Nos. NSC-98-2112-M-009-011-MY2, NSC-97-2120-M009-004, and NSC97-2221-E009-161. S.J.C also would like to thank the National Center of Theoretical Sciences in Hsinchu and the National Center for High-Performance Computing of Taiwan for supporting.

*sjcheng@mail.nctu.edu.tw

[1] D. Gammon, E. S. Snow, B. V. Shanabrook, D. S. Katzer, and D. Park, Phys. Rev. Lett. **76**, 3005 (1996).
[2] A. S. Bracker, D. Gammon, and V. L. Korenev, Semicond. Sci. Technol. **23**, 114004 (2008).
[3] C. Santori, D. Fattal, M. Pelton, G. S. Solomon, and Y. Yamamoto, Phys. Rev. B **66**, 045308 (2002).
[4] K. Edamatsu, Jpn. J. Appl. Phys., Part 1 **46**, 7175 (2007).
[5] E. L. Ivchenko, Phys. Status Solidi A **164**, 487 (1997).
[6] T. Takagahara, Phys. Rev. B **62**, 16840 (2000).
[7] R. M. Stevenson, R. J. Young, P. Atkinson, K. Cooper, D. A. Ritchie, and A. J. Shields, Nature (London) **439**, 179 (2006).
[8] N. Akopian, N. H. Lindner, E. Poem, Y. Berlatzky, J. Avron, D. Gershoni, B. D. Gerardot, and P. M. Petroff, Phys. Rev. Lett. **96**, 130501 (2006).
[9] R. Hafenbrak, S. M. Ulrich, P. Michler, L. Wang, A. Rastelli, and O. G. Schmidt, New J. Phys. **9**, 315 (2007).
[10] M. Bayer, G. Ortner, O. Stern, A. Kuther, A. A. Gorbunov, A. Forchel, P. Hawrylak, S. Fafard, K. Hinzer, T. L. Reinecke, S. N. Walck, J. P. Reithmaier, F. Klopf, and F. Schäfer, Phys. Rev. B **65**, 195315 (2002).
[11] W. Langbein, P. Borri, U. Woggon, V. Stavarache, D. Reuter, and A. D. Wieck, Phys. Rev. B **69**, 161301(R) (2004).
[12] A. Greilich, M. Schwab, T. Berstermann, T. Auer, R. Oulton, D. R. Yakovlev, M. Bayer, V. Stavarache, D. Reuter, and A. Wieck, Phys. Rev. B **73**, 045323 (2006).
[13] B. D. Gerardot, S. Seidl, P. A. Dalgarno, R. J. Warburton, D. Granados, J. M. Garcia, K. Kowalik, O. Krebs, K. Karrai, A. Badolato, and P. M. Petroff, Appl. Phys. Lett. **90**, 041101 (2007).
[14] M. E. Reimer, M. Korkusiński, D. Dalacu, J. Lefebvre, J. Lapointe, P. J. Poole, G. C. Aers, W. R. McKinnon, P. Hawrylak, and R. L. Williams, Phys. Rev. B **78**, 195301 (2008).
[15] R. J. Young, R. M. Stevenson, A. J. Shields, P. Atkinson, K. Cooper, D. A. Ritchie, K. M. Groom, A. I. Tartakovskii, and M. S. Skolnick, Phys. Rev. B **72**, 113305 (2005).
[16] R. Seguin, A. Schliwa, S. Rodt, K. Potschke, U. W. Pohl, and D. Bimberg, Phys. Rev. Lett. **95**, 257402 (2005).
[17] M. Abbarchi, C. A. Mastrandrea, T. Kuroda, T. Mano, K. Sakoda, N. Koguchi, S. Sanguinetti, A. Vinattieri, and M. Gurioli, Phys. Rev. B **78**, 125321 (2008).
[18] M. C. Xu, Y. Temko, T. Suzuki, and K. Jacobi, J. Appl. Phys. **98**, 083525 (2005).
[19] W. H. Chang, H. Lin, S. Y. Wang, C. H. Lin, S. J. Cheng, M. C. Lee, W. Y. Chen, T. M. Hsu, T. P. Hsieh, and J. I. Chyi, Phys. Rev. B **77**, 245314 (2008).
[20] R. M. Stevenson, R. J. Young, P. See, D. G. Gevaux, K. Cooper, P. Atkinson, I. Farrer, D. A. Ritchie, and A. J. Shields, Phys. Rev. B **73**, 033306 (2006).
[21] COMSOL multiphysics package.
[22] O. Stier, M. Grundmann, and D. Bimberg, Phys. Rev. B **59**, 5688 (1999).
[23] O. Gunawan, H. S. Djie, and B. S. Ooi, Phys. Rev. B **71**, 205319 (2005).

[24] Y. Wang, H. S. Djie, and B. S. Ooi, Appl. Phys. Lett. **89**, 151104 (2006).
[25] M. F. Tsai, H. Lin, C. H. Lin, S. D. Lin, S. Y. Wang, M. C. Lo, S. J. Cheng, M. C. Lee, and W. H. Chang, Phys. Rev. Lett. **101**, 267402 (2008).
[26] E. Poem, J. Shemesh, I. Marderfeld, D. Galushko, N. Akopian, D. Gershoni, B. D. Gerardot, A. Badolato, and P. M. Petroff, Phys. Rev. B **76**, 235304 (2007).
[27] Y. Léger, L. Besombes, L. Maingault, and H. Mariette, Phys. Rev. B **76**, 045331 (2007).
[28] M. M. Glazov, E. L. Ivchenko, O. Krebs, K. Kowalik, and P. Voisin, Phys. Rev. B **76**, 193313 (2007).
[29] I. Vurgaftman, J. R. Meyer, and L. R. Ram-Mohan, J. Appl. Phys. **89**, 5815 (2001).
[30] H. Htoon, M. Furis, S. A. Crooker, S. Jeong, and V. I. Klimov, Phys. Rev. B **77**, 035328 (2008).